Available online at www.sciencedirect.com
SCIENCE DIRECT®
Journal of Luminescence 110 (2004) 135–145
JOURNAL OF LUMINESCENCE
www.elsevier.com/locate/jlumin

Low-temperature high-resolution VUV spectroscopy of Ce^{3+} doped $LiYF_4$, $LiLuF_4$ and LuF_3 crystals

N.Yu. Kirikova[a], M. Kirm[b], J.C. Krupa[c], V.N. Makhov[a,*], E. Negodin[b], J.Y. Gesland[d]

[a] *Lebedev Physical Institute, Leninsky Prospect 53, 119991 Moscow, Russia*
[b] *Institut für Experimentalphysik der Universität Hamburg, 22761 Hamburg, Germany*
[c] *Institut de Physique Nucléaire, 91406 Orsay Cedex, France*
[d] *Université du Maine, 72017 Le Mans, France*

Received 17 December 2003; received in revised form 6 May 2004; accepted 6 May 2004

Available online 2 July 2004

Abstract

For $LiYF_4:Ce^{3+}$, $LiLuF_4:Ce^{3+}$ and $LuF_3:Ce^{3+}$ crystals UV/visible emission and time-resolved VUV/UV excitation spectra were recorded at liquid helium temperature with spectral resolution of 0.1 nm for excitation spectra and better than 0.3 nm for emission spectra. Well resolved fine structures due to zero-phonon lines were clearly observed in both excitation and emission spectra for $LiYF_4:Ce^{3+}$ and $LiLuF_4:Ce^{3+}$. For $LuF_3:Ce^{3+}$ crystal no fine structure was detected in the spectra even at the highest spectral resolution. Under the host excitation, the fine structure for high-energy emission band of Ce^{3+} ($5d–{}^2F_{5/2}$) in $LiLuF_4:Ce^{3+}$ becomes well pronounced because of weaker reabsorption effect, as compared to Ce^{3+} 4f–5d absorption, due to small penetration depth for exciting radiation. As a result the crystal-field splitting for ${}^2F_{7/2}$ and ${}^2F_{5/2}$ levels of Ce^{3+} in $LiLuF_4$ crystal was measured. First observation of zero-phonon lines at $\sim$81,550 and $\sim$82,900 cm^{-1} as well as vibronic side bands due to interconfigurational $4f^{14}–4f^{13}5d$ transitions in Lu^{3+} is reported for excitation spectrum of $LiLuF_4:Ce^{3+}$.

PACS: 78.55; 78.60; 78.40; 78.47; 42.70.H

Keywords: 5d–4f luminescence; Trivalent cerium and lutetium; Fluoride crystals

1. Introduction

$LiYF_4:Ce^{3+}$ and $LiLuF_4:Ce^{3+}$ crystals are well known luminescent materials which were extensively studied from the viewpoint of their possible applications for solid-state lasers [1–3] and neutron scintillation detectors [4–5]. On the other hand, these wide band-gap materials doped with different rare earth (RE) ions were used as model systems for spectroscopic studies of high-energy levels of REs in crystalline environment with the

*Corresponding author. Fax: +7-095-938-2251.
E-mail address: makhov@sci.lebedev.ru (V.N. Makhov).

0022-2313/$ - see front matter © 2004 Elsevier B.V. All rights reserved.
doi:10.1016/j.jlumin.2004.05.002

technique of VUV spectroscopy [6–10]. VUV spectroscopic research of these materials was stimulated also by strong commercial interest in new efficient VUV-excited phosphors for mercury-free fluorescent tubes and plasma display panels [11,12].

$LiYF_4$ and $LiLuF_4$ are examples of the crystals with intermediate electron-lattice coupling for 4f–5d transitions in doping RE ions when along wide vibronic bands the narrow zero-phonon lines are observed [13,14]. The latter is very important for the identification of levels and electronic transitions in RE ions. Moreover, as was shown in [13,14], the disappearance of this fine structure for a particular higher-energy 4f–5d excitation band indicates that the corresponding 5d level of the RE ion is situated above the energy gap of the host crystal that leads to autoionization of the respective level of RE ion and accordingly the 5d level becomes broadened due to short lifetime. In some cases the fine structure due to zero-phonon lines reappears at high energies but this effect can be observed only for RE ions with more than one 4f electron [15]. For LuF_3 crystals doped with RE ions no zero-phonon lines were observed so far by any authors and accordingly it is supposed that this crystal possesses stronger electron-lattice coupling for 4f–5d transitions in doping RE ions than $LiYF_4$ and $LiLuF_4$.

The Ce^{3+} ion has only one 4f electron in the ground configuration. In the excited configuration of Ce^{3+} there is one 5d electron with empty 4f shell. So, the structure of the 4f–5d transitions will be dominated by crystal-field splitting of the 5d states of Ce^{3+}, since there is no interaction within 4f core and interaction between 4f core and 5d electron for Ce^{3+} which strongly influence the energy level structure for excited configuration of RE ions with more than one 4f electron [13,14]. Due to this reason, excitation spectrum of Ce^{3+} 5d–4f emission for $LiYF_4$:Ce^{3+} and $LiLuF_4$:Ce^{3+} crystals, at its lowest-energy edge of 4f–5d absorption, should consist of one zero-phonon line and wide vibronic side band which can be superimposed by some narrow vibronic lines. The Lu^{3+} ion has completely filled 4f shell in its ground configuration $4f^{14}$, but its excited configuration $4f^{13}5d$ is equivalent to some extent to that of Pr^{3+} ion 4f5d. The edge of $4f^{14}$–$4f^{13}5d$ transitions in Lu^{3+} is situated at energies $>80{,}000\,cm^{-1}$ [16], and for the observation of these transitions it is necessary to have the host with very wide band gap. This requirement is fulfilled for $LiYF_4$ and $LiLuF_4$ crystals.

In the present paper low-temperature emission spectra in the UV/visible range and time-resolved excitation spectra in the VUV/UV range have been studied with high spectral resolution for $LiYF_4$:Ce^{3+}, $LiLuF_4$:Ce^{3+} and LuF_3:Ce^{3+} crystals with the aim of comparing luminescence properties of these Ce^{3+} doped Y^{3+}- and Lu^{3+}-based compounds.

2. Experiment

The studies of emission and excitation spectra as well as luminescence decay kinetics were performed at the SUPERLUMI station [17] of HASYLAB at DESY (Hamburg) under pulsed excitation by 50–320 nm synchrotron radiation from the DORIS storage ring. Excitation spectra were measured with an instrumental resolution as high as 0.1 nm. Luminescence spectra in the UV and visible range were recorded with a 0.3 m Czerny-Turner-type secondary monochromator-spectrograph SpectraPro-308 (Acton Research Corporation) equipped with a liquid nitrogen cooled CCD detector (Princeton Instruments, Inc.). The spectral resolution of the analyzing monochromator with the 1200 grooves/mm grating was better than 0.3 nm. Luminescence spectra were not corrected for the spectral response of the detection system. For excitation spectra measurements as well as for time-resolved measurements (with a time resolution of 0.8 ns) the luminescence was detected by a photomultiplier (Hamamatsu R6358P).

$LiLuF_4$ and LuF_3 single crystals doped with 0.1 at% of cerium and $LiYF_4$ single crystal doped with 1.0 at% of cerium were grown by the Czochralski method or the Stockbarger–Bridgman technique as described in [18]. The concentrations of Ce^{3+} indicated are those in the melt. The real concentrations of Ce^{3+} in the crystals were not measured and can be slightly lower. The crystal

structure of $LiYF_4$ and $LiLuF_4$ is inverse scheelite structure, space group $I4_1/a$, and the site symmetry for Y^{3+} (Lu^{3+}) ions is S_4. The coordination number for Y^{3+} (Lu^{3+}) sites is 8. The LuF_3 crystal has a rather complicated crystal lattice (orthorhombic YF_3 structure) where each Lu^{3+} ion is surrounded by 9 fluorine ligands.

The crystals were cleaved before the installation onto the sample holder in a liquid helium cryostat. The crystallographic axes of the crystals were not oriented with respect to polarization vector of synchrotron radiation.

3. Results and discussion

Fig. 1 shows emission spectra of $LiYF_4:Ce^{3+}$, $LiLuF_4:Ce^{3+}$ and $LuF_3:Ce^{3+}$ crystals. Two broad bands are observed in emission spectra which are due to transitions from the lowest 5d level of Ce^{3+} to $^2F_{5/2}$ and $^2F_{7/2}$ states of Ce^{3+} 4f ground

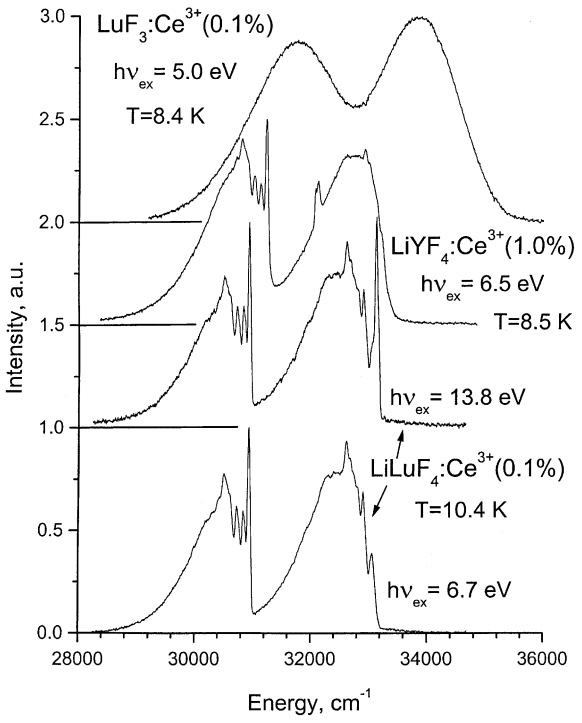

Fig. 1. High-resolution emission spectra of $LiYF_4:Ce^{3+}$, $LiLuF_4:Ce^{3+}$ and $LuF_3:Ce^{3+}$ crystals under excitation by photons with different energies.

configuration. The energy separation between the bands agrees with the value of the spin-orbit splitting (of the order $2000\,cm^{-1}$) for the ground $^2F_{5/2,7/2}$ state of Ce^{3+} ion. For $LiYF_4:Ce^{3+}$ and $LiLuF_4:Ce^{3+}$ crystals the emission bands consist of sharp zero-phonon lines and broad vibronic sidebands. The lines near 310 nm ($32{,}250\,cm^{-1}$) in the spectrum of $LiYF_4:Ce^{3+}$ are due to emission of spurious traces of Gd^{3+} ions in the crystal . The fine structure is less pronounced for the higher-energy emission band. This effect is usually ascribed to reabsorption of emitting radiation [13]. However, under higher-energy excitation of the $LiLuF_4:Ce^{3+}$ crystal (under the host absorption) the sharp lines in the higher-energy band become well pronounced. In accordance with the reabsorption model this can be explained by a smaller penetration depth for the exciting radiation under the host absorption compared to absorption by the Ce^{3+} ions that results in weaker reabsorption of Ce^{3+} emission. Three sharp lines in the higher-energy band and four sharp lines in the lower-energy band dominate over other features in the emission spectrum of $LiLuF_4:Ce^{3+}$ crystal and can be ascribed to crystal-field components in the S_4 symmetry of the $^2F_{5/2}$ and $^2F_{7/2}$ ground state levels of Ce^{3+} respectively.

Similar effect at high-energy excitation was not detected for the $LiYF_4:Ce^{3+}$ crystal, probably because of higher concentration of Ce^{3+} in this crystal. However, it should be mentioned that the energy separation between sharp lines in emission spectrum of $LiYF_4:Ce^{3+}$ and of $LiLuF_4:Ce^{3+}$ is absolutely the same (within the measurement accuracy) including all four lines in the lower-energy band and the only well-pronounced line for $LiYF_4:Ce^{3+}$ in the higher-energy band. This can be expected for crystal-field splitting of the Ce^{3+} 4f levels $^2F_{5/2}$ and $^2F_{7/2}$ because of very similar lattice parameters for $LiYF_4$ and $LiLuF_4$ crystals. However, the emission spectrum for the $LiLuF_4:Ce^{3+}$ crystal is totally shifted to lower energies by $\sim 300\,cm^{-1}$ compared to that for the $LiYF_4:Ce^{3+}$ crystal, and this value should be considered as the energy difference between the lowest Ce^{3+} 5d levels in $LiYF_4:Ce^{3+}$ and $LiLuF_4:Ce^{3+}$.

The weaker structure is also observed in emission spectra of $LiYF_4:Ce^{3+}$ and $LiLuF_4:Ce^{3+}$ arising from the phonon satellites of zero-phonon lines but this structure is smeared because several phonon modes are involved in electron–phonon interaction. In the spectrum of $LuF_3:Ce^{3+}$ both emission bands have a smooth Gaussian-like shape, and no zero-phonon lines were detected in the spectrum even at the highest spectral resolution used in the present study. This was actually expected for both emission and excitation spectrum of $LuF_3:Ce^{3+}$ because of much stronger electron–phonon interaction between 5d states of RE^{3+} ions and lattice vibrations in this crystal as compared to $LiYF_4:Ce^{3+}$ and $LiLuF_4:Ce^{3+}$. That results in larger Stokes shift between absorption and emission for 4f–5d transitions in RE^{3+} ions and accordingly zero-phonon lines do not appear in the spectra.

Fig. 2 shows the excitation spectra of Ce^{3+} 5d–4f emission in $LiYF_4:Ce^{3+}$, $LiLuF_4:Ce^{3+}$ and $LuF_3:Ce^{3+}$ crystals. Five broad bands are observed in the spectral range 33,000–56,000 cm^{-1} for $LiYF_4:Ce^{3+}$ and $LiLuF_4:Ce^{3+}$ crystals and 36,000–55,000 cm^{-1} for $LuF_3:Ce^{3+}$ crystal which are due to transitions from the ground 4f $^2F_{5/2}$ level of Ce^{3+} to crystal-field levels of the Ce^{3+} 5d excited configuration. Contrary to the case of $LiYF_4:Ce^{3+}$ the maxima of the lowest-energy band and of three higher-energy 4f–5d bands (at 47,000–56,000 cm^{-1}) in the spectrum of $LiLuF_4:Ce^{3+}$ are seen as dips, probably due to very high absorption coefficient causing the saturation of Ce^{3+} 4f–5d transitions in this spectral range. The reason that this effect is well pronounced for the $LiLuF_4:Ce^{3+}$ sample with lower Ce^{3+} concentration but is not observed for the $LiYF_4:Ce^{3+}$ sample with higher Ce^{3+} concentration is not clear. Possible explanation could be that the real concentrations of Ce^{3+} in the crystals are not the same as in the melt. The shape of excitation spectrum can be also influenced by the thickness of samples, which was different for the studied crystals, and by the orientation of crystallographic axis of the crystals with respect to polarization of incident radiation.

In the spectrum of $LuF_3:Ce^{3+}$ the onset of 4f–5d transitions occurs at much higher energy

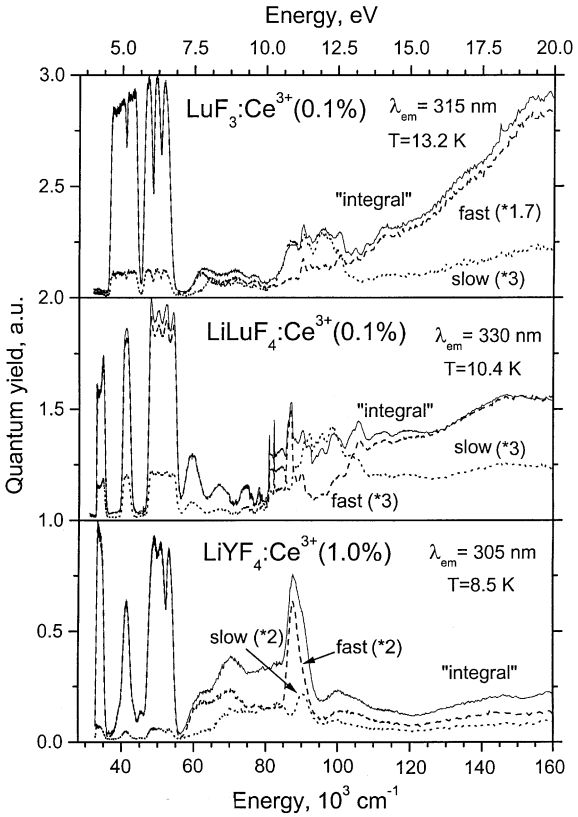

Fig. 2. Time-resolved and time-integrated excitation spectra of Ce^{3+} 5d–4f emission in $LiYF_4:Ce^{3+}$, $LiLuF_4:Ce^{3+}$ and $LuF_3:Ce^{3+}$ crystals. The time windows and the delay with respect to excitation pulse of synchrotron radiation were: (a) for the detection of the fast component: 23 and 0 ns; 15.5 and 1.3 ns; 21.7 and 1.2 ns; (b) for the detection of the slow component: 63.8 and 23 ns; 102 and 60 ns; 93 and 68 ns; for $LiYF_4:Ce^{3+}$, $LiLuF_4:Ce^{3+}$ and $LuF_3:Ce^{3+}$ crystals, respectively.

and the energy range over which the Ce^{3+} 5d crystal-field levels are spread is narrower than in $LiYF_4:Ce^{3+}$ and $LiLuF_4:Ce^{3+}$ that should be expected by taking into account the crystal-field magnitude variation with coordination number for RE sites, namely higher coordination number (9) in LuF_3 than in $LiYF_4$ and $LiLuF_4$ (8). For two lowest-energy 4f–5d bands in the excitation spectrum of the $LuF_3:Ce^{3+}$ crystal there are also dips in the maxima of the bands, but not so well pronounced as in the case of $LiLuF_4:Ce^{3+}$ crystal.

The fine structure clearly observed at the edge of the lowest-energy band for $LiYF_4:Ce^{3+}$ and

$LiLuF_4:Ce^{3+}$ is shown in more details in Fig. 3. Excitation spectrum of the $LiYF_4:Ce^{3+}$ crystal is very similar to those obtained before in Ref. [13] and starts with single zero-phonon line (at 33,450 cm^{-1}) expected for the Ce^{3+} ion with only one 5d electron in its excited configuration. On the high-energy side rather weak structure superimposed on the wide vibronic side-band of this zero-phonon line can be distinguished, arising from vibronic lines. This structure is not well resolved and it is difficult to characterize quantitatively phonon frequencies of these vibrations.

As was mentioned before, in the excitation spectrum of the $LiLuF_4:Ce^{3+}$ crystal the maxima of absorption by 4f–5d transitions in Ce^{3+} correspond to minima in the excitation spectrum, i.e. we should locate zero-phonon line at 33,130 cm^{-1}. Besides two more well resolved narrow dips at 33,180 and 33,265 cm^{-1} can be distinguished in the spectrum. These two lines separated from the first zero-phonon line by 50 and $\sim$135 cm^{-1} can be due to phonon satellites of zero-phonon line. Most probably these are some local vibrations with small phonon energies in which heavy Ce^{3+} ions are involved, since the energies of any intrinsic lattice vibrations in $LiLuF_4$ should definitely exceed 100 cm^{-1} [19]. The shape of this part of the spectrum (the relative positions of main features) for the $LiLuF_4:Ce^{3+}$ crystal does not resemble the threshold area of the spectrum for the $LiYF_4:Ce^{3+}$ crystal. Obviously different vibrational modes are involved in electron–phonon interaction between the lowest 5d-state of Ce^{3+} and the lattice vibrations in $LiYF_4:Ce^{3+}$ and $LiLuF_4:Ce^{3+}$ crystals. It should be also mentioned that the energy separations between narrow lines in the excitation spectrum of the $LiLuF_4:Ce^{3+}$ crystal are different than those observed in the emission spectrum of this crystal. This seems to confirm the conclusion that narrow lines in emission spectra of $LiYF_4:Ce^{3+}$ and $LiLuF_4:Ce^{3+}$ crystals are zero-phonon lines corresponding to the transitions to crystal-field levels of the Ce^{3+} $^2F_{5/2}$ and $^2F_{7/2}$ multiplets whereas the fine structure in the excitation spectra is due to single zero-phonon line and phonon satellites.

As shown in Fig. 2, in the spectral range 56,000–81,000 cm^{-1} several broad and weaker excitation bands are observed in all three crystals which can be due to transitions to higher-energy (6s, 6p) states of Ce^{3+} [20] or/and to the absorption by some defects or impurities. In particular, in the spectrum of $LiLuF_4:Ce^{3+}$ crystal where the concentration of Ce^{3+} was quite low (0.1 at%) the fine structure can be seen with the edges at $\sim$70,500, $\sim$76,000 and $\sim$79,000 cm^{-1} ($\sim$8.8, $\sim$9.5 and

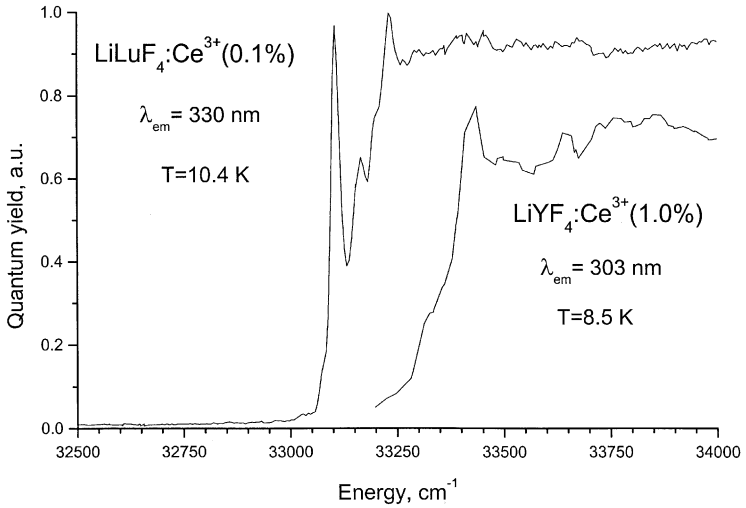

Fig. 3. A comparison of excitation spectra of Ce^{3+} 5d–4f emission in $LiYF_4:Ce^{3+}$ and $LiLuF_4:Ce^{3+}$ in the region near the edge of Ce^{3+} 4f–5d absorption.

$\sim$9.9 eV respectively), which is due to absorption by spurious traces of other RE ions present in the crystal, most probably to 4f–5d absorption by Yb^{3+} and maybe Gd^{3+} [14,21]. This structure appears in the excitation spectra of Ce^{3+} emission as narrow dips, since absorption by these ions is a competing process and does not result in Ce^{3+} emission. The onset of 4f–5d absorption by traces of Tb^{3+} in this crystal is also seen in the spectrum as a narrow and very weak peak at $\sim$46,200 cm^{-1} ($\sim$5.8 eV).

At photon energies $>$81,000 cm^{-1} (10.1 eV) in excitation spectra of $LiLuF_4$:Ce^{3+} and LuF_3:Ce^{3+} crystals a new feature appears: an increase of intensity of Ce^{3+} emission with a sharp edge and fine structure for the $LiLuF_4$:Ce^{3+} crystal and with a smooth shape for the LuF_3:Ce^{3+} crystal. The fine structure in the spectrum of the $LiLuF_4$:Ce^{3+} crystal is shown in more details in Fig. 4. In the excitation spectrum of $LiYF_4$:Ce^{3+} no any remarkable features are observed in this spectral range until photon energies $\sim$85,500 cm^{-1} ($\sim$10.7 eV) where relatively wide band of strong Ce^{3+} emission appears. At the same energies the increase of Ce^{3+} emission intensity is also observed in the spectrum of $LiLuF_4$:Ce^{3+}, but the band is more narrow than in the case of $LiYF_4$:Ce^{3+}. At higher photon energies rather rich structure is observed in excitation spectra of both Lu^{3+}-based crystals until the energies $\sim$120,000 cm^{-1} ($\sim$15 eV). The excitation spectrum of the Ce^{3+} emission from the $LiYF_4$:Ce^{3+} crystal is smooth and structureless in this spectral range.

The decay curves for Ce^{3+} 5d–4f emission from $LiYF_4$:Ce^{3+} and $LiLuF_4$:Ce^{3+} crystals under the excitation by photons with different energies are shown in Fig. 5. Under the Ce^{3+} 4f–5d excitation the decay is single-exponential and decay times of Ce^{3+} 5d–4f emission are practically the same for $LiYF_4$:Ce^{3+} and $LiLuF_4$:Ce^{3+}: 28.61 ± 0.04 and 28.58 ± 0.03 ns respectively. Under the higher-energy excitation the decay becomes non-exponential and the shape of decay curves under different excitation energies indicate that there exists more than one mechanism of the energy transfer to Ce^{3+} ions. In the excitation spectra of $LiLuF_4$:Ce^{3+} and LuF_3:Ce^{3+}, in the range starting from 81,000 cm^{-1} up to $\sim$120,000 cm^{-1} (10–15 eV) the fraction of the slow component is larger and the fast and slow components show the anticorrelated behavior. This feature reflects a

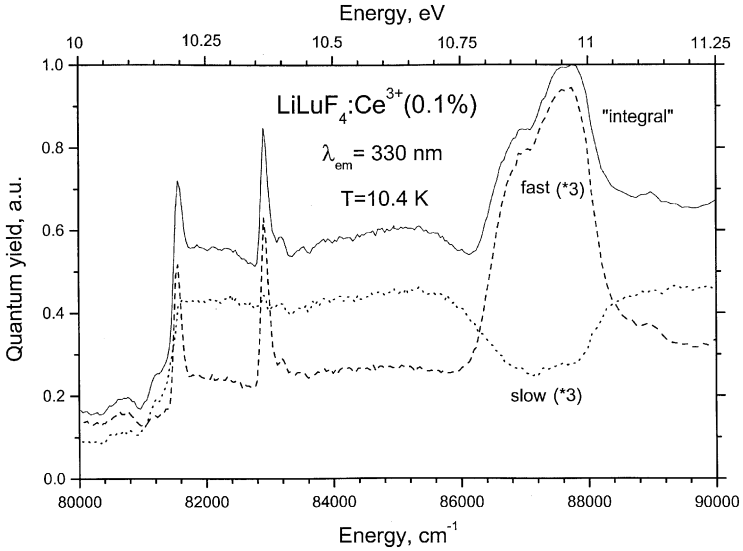

Fig. 4. Time-resolved and time-integrated excitation spectra of Ce^{3+} 5d–4f emission in $LiLuF_4$:Ce^{3+} in the region near the edge of Lu^{3+} $4f^{14}$–$4f^{13}5d$ absorption. The time windows and the delay with respect to excitation pulse of synchrotron radiation were: for the detection of the fast component: 15.5 and 1.3 ns; for the detection of the slow component: 102 and 60 ns, respectively.

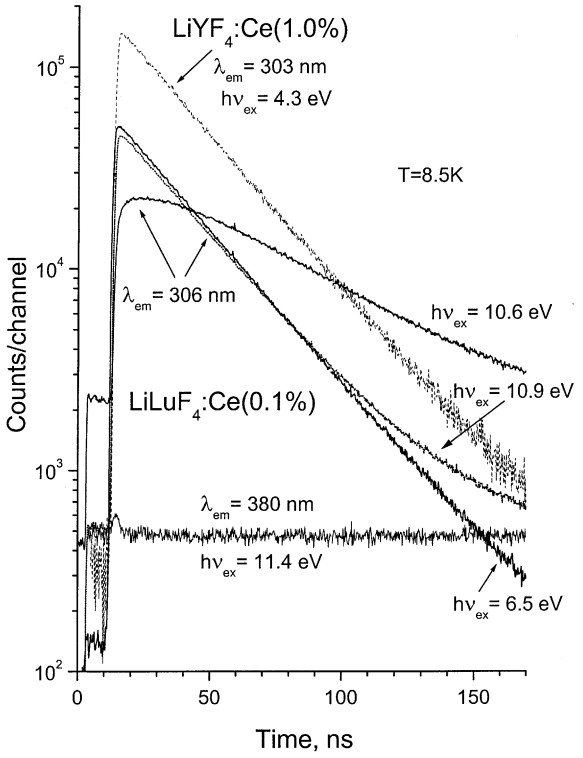

Fig. 5. Decay curves of Ce^{3+} 5d–4f emission from $LiYF_4:Ce^{3+}$ (upper curve, dashed line) and $LiLuF_4:Ce^{3+}$ (lower curves, solid and dotted lines) and of 380 nm (3.2 eV) emission from the $LiLuF_4:Ce^{3+}$ crystal (the lowest curve).

competition between two channels of the energy transfer to Ce^{3+} ions, namely the fast and the slow. It will be supposed that the slow channel corresponds to well-known mechanisms of the energy transfer from the host to Ce^{3+} ions (recombinational or excitonic) whereas Lu^{3+} ions are responsible for the fast channel.

By taking into account the results from Ref. [16], the overall consideration of all spectral-kinetic features observed in the studied materials, especially in the excitation spectra, allows us to conclude that absorption by Lu^{3+} ions starts at photon energies $>81{,}000\,cm^{-1}$ but not at 8 eV ($64{,}000\,cm^{-1}$) as proposed in [22]. Thus, we ascribe two narrow lines observed in the excitation spectrum of $LiLuF_4:Ce^{3+}$ at $>81{,}000\,cm^{-1}$ to zero-phonon lines which are due to interconfigurational $4f^{14}$–$4f^{13}5d$ transitions in Lu^{3+}. The broad bands situated at the high-energy side of these lines are (at least partly) assigned to the vibronic side bands. Following the methodology of Ref. [23] for the prediction of the energy for the lowest $4f^{13}5d$ level of Lu^{3+} in a particular host the energy of the Lu^{3+} low-spin 5d state in $LiLuF_4$ (the energy of the lowest-energy spin-allowed $4f^{14}$–$4f^{13}5d$ transitions in Lu^{3+}) should be $\sim 82{,}300\,cm^{-1}$ which is in rather good agreement with the energies of the sharp lines observed in the excitation spectrum of $LiLuF_4:Ce^{3+}$, particularly by taking into account that almost no experimental data is available for the $4f^{14}$–$4f^{13}5d$ transitions in Lu^{3+} ion. The energy separation between two lines is $\sim 1350\,cm^{-1}$. This energy difference corresponds to the energy splitting between low-spin and high-spin 5d states of Lu^{3+}, being in agreement with common tendency in decreasing this value observed from Tb^{3+} to Yb^{3+} and that in Yb^{3+} this splitting is of the order $1500\,cm^{-1}$ [14]. Due to high concentration (100%) of Lu^{3+} in the crystal, absorption on the spin-forbidden Lu^{3+} $4f^{14}$–$4f^{13}5d$ transitions to high-spin Lu^{3+} 5d state can in principle become as strong as on spin-allowed transitions to low-spin Lu^{3+} 5d state and therefore is well pronounced in the spectra. On the other hand, these two zero-phonon lines can be also due to transitions to different sub-bands in the lowest-energy Lu^{3+} 5d crystal-field component, which are usually observed for RE ions with more than one 4f electron and appear due to Coulomb interaction between 4f and 5d electrons [13,14]. For comparison the energy separation between first and second sub-bands within the lowest 5d crystal-field component of Pr^{3+} doped into $LiYF_4$ is $1625\,cm^{-1}$ [13]. The choice between these two possibilities needs further experimental as well as theoretical studies.

On the high-energy side of both sharp lines observed at $>81{,}000\,cm^{-1}$ and ascribed to zero-phonon lines of Lu^{3+} $4f^{14}$–$4f^{13}5d$ transitions the weak structure can be distinguished (see Fig. 4) which can be due to vibronic satellites of these zero-phonon lines. The energy separation between neighbors for these weak lines lies in the range 240–350 cm^{-1} and no periodic structure can be found. This is an indication that more than one phonon mode is involved in electron–phonon interaction between the lowest 5d-state of Lu^{3+} and the lattice vibrations in the $LiLuF_4$ crystal,

however the phonon energies corresponds well to intrinsic vibrations of the lattice.

The absence of fine structure due to zero-phonon lines at the edge of Lu^{3+} $4f^{14}$–$4f^{13}5d$ transitions in excitation spectrum of $LuF_3:Ce^{3+}$ has obviously the same nature as at the edge of Ce^{3+} 4f–5d transitions and is due to much stronger electron–phonon interaction between 5d states of Lu^{3+} ions and lattice vibrations in this crystal as compared to $LiLuF_4:Ce^{3+}$.

As was already mentioned above [13,14], for the observation of fine structure (zero-phonon lines) in 4f–5d transitions it is necessary that the corresponding 5d level is located below the bottom of the conduction band, otherwise the lines will be broadened due to their short lifetime caused by autoionization. The wide band in excitation spectrum of $LiLuF_4:Ce^{3+}$ with the edge at $\sim 86{,}000\,cm^{-1}$ can indicate just the threshold for autoionization of the $4f^{13}5d$ levels of Lu^{3+}. Since the peak of reflection (absorption) spectrum corresponding to the creation of F^-2p exciton in the $LiYF_4$ crystal is situated at 11.5 eV ($92{,}000\,cm^{-1}$) [24], the energy gap for this crystal can be estimated as being ~ 12.5 eV ($100{,}000\,cm^{-1}$). Similar energy gap corresponding to band-to-band transitions from the F^-2p valence band to the conduction band can be expected for the $LiLuF_4$ crystal. So, we can locate the ground $4f^{14}$ ($^1S_0$) state of Lu^{3+} in $LiLuF_4$ crystal at ~ 1.75 eV ($14{,}000\,cm^{-1}$) above the top of the valence band. For Ce^{3+} 4f–5d transitions in $LiLuF_4:Ce^{3+}$ and $LiYF_4:Ce^{3+}$ the second crystal-field component in excitation spectra at $\sim 40{,}000\,cm^{-1}$ has already no fine structure, that can be due to lifetime broadening if the corresponding 5d level is situated in the conduction band. Based on this assumption the ground 4f level of Ce^{3+} in these crystals can be located at $\sim 60{,}000\,cm^{-1}$ above the top of the F^-2p valence band. The deduced energy bands of $LiLuF_4$ crystal and the positions of Lu^{3+} and Ce^{3+} energy levels in the energy gap of this crystal are schematically shown in Fig. 6. Of course this scheme can be considered as only rough approximation. In particular, the obtained position of the ground 4f level of Ce^{3+} is not consistent with that observed in CeF_3 and $LaF_3:Ce^{3+}$ where the ground 4f level of Ce^{3+} is located only at about 4 eV ($\sim 32{,}000\,cm^{-1}$) above the top of the valence band [25]. One of the reasons can be that we overestimated the energy gap value for $LiLuF_4$. On the other hand, the ground 4f level of Ce^{3+} in such a wide-band matrix as CaF_2 was obtained to be at about 6 eV ($\sim 48{,}000\,cm^{-1}$) above the valence band [26] that is closer to the value obtained here for $LiLuF_4:Ce^{3+}$ and $LiYF_4:Ce^{3+}$. In any case the relative energy positions of the ground 4f states for

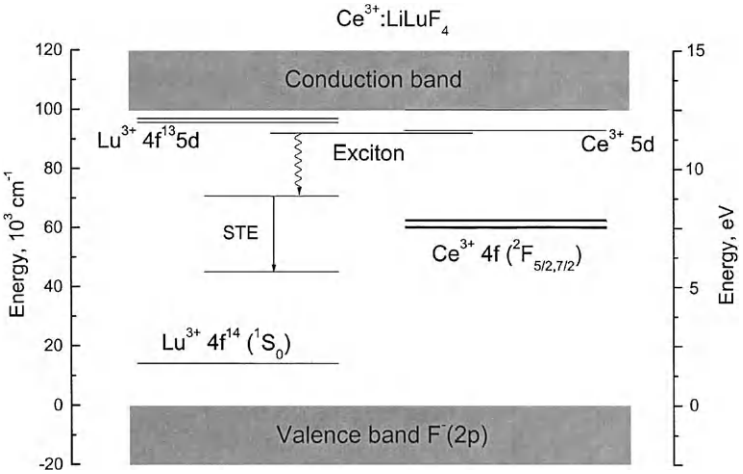

Fig. 6. Energy band scheme for $LiLuF_4$ crystal and the positions of 4f and 5d energy levels of Lu^{3+} and Ce^{3+} in the energy gap of this crystal.

Lu^{3+} and Ce^{3+} in the energy gap of the $LiLuF_4$ matrix are in line with the common tendency for 4f ground states of RE ions relative to the host bands [26,27].

As was already mentioned in [22] the energy position of the Lu^{3+} 4f ground state slightly above the top of the valence band can enhance the capture of thermalized holes by Ce^{3+} ions via Lu^{3+} ions that can explain higher efficiency of the energy transfer from the host to Ce^{3+} in $LiLuF_4$:Ce^{3+} than in $LiYF_4$:Ce^{3+}.

In the energy range 86,000–104,000 cm^{-1} (10.75–13 eV) the structure in excitation spectra of $LiLuF_4$:Ce^{3+} and LuF_3:Ce^{3+} reflects the features in absorption and reflection spectra observed in the low-energy part of the fundamental absorption by the host containing Lu^{3+}. Such features in the reflection spectrum of similar material $KLuF_4$ as compared to KYF_4 were observed already [28]. Excitation spectra show the anticorrelated behavior with respect to absorption (reflection) spectrum due to near-surface nonradiative losses of excitations because of very high absorption coefficient of the host in this spectral region. On the other hand, the spectral range 10–13 eV (81,000–104,000 cm^{-1}) should correspond to the region of interconfigurational $4f^{14}$–$4f^{13}5d$ transitions in Lu^{3+} which overlaps with excitonic absorption at $h\nu \sim 11.5$ eV and absorption on band-to-band transitions from the F^-2p valence band at $h\nu > 12.5$ eV. As a result, several channels of the energy transfer to Ce^{3+} ions may occur simultaneously (with different efficiency depending on the photon energy) leading to rather complicated time behavior of Ce^{3+} 5d–4f emission in this spectral range. It is important to note that this spectral range is wider for $LiLuF_4$:Ce^{3+} than for LuF_3:Ce^{3+} in agreement with the observation of spectral widths covered by Ce^{3+} 4f–5d transitions to different 5d crystal-field levels of Ce^{3+} in these matrices.

At excitation photon energies >11.2 eV (90,000 cm^{-1}) the wide-band emission peaked near 380 nm (3.2 eV) is observed from the $LiLuF_4$:Ce^{3+} crystal (Fig. 7). Since this emission is excited only in the region of fundamental absorption by the host, it can be ascribed to luminescence of self-trapped excitons (STE) in $LiLuF_4$. The excitation edge of this emission is located on the long-wavelength tail of excitonic absorption and emission intensity decreases remarkably at photon energies exceeding the edge of band-to-band transitions, as it is usually observed for such kind of luminescence. The wide emission band of

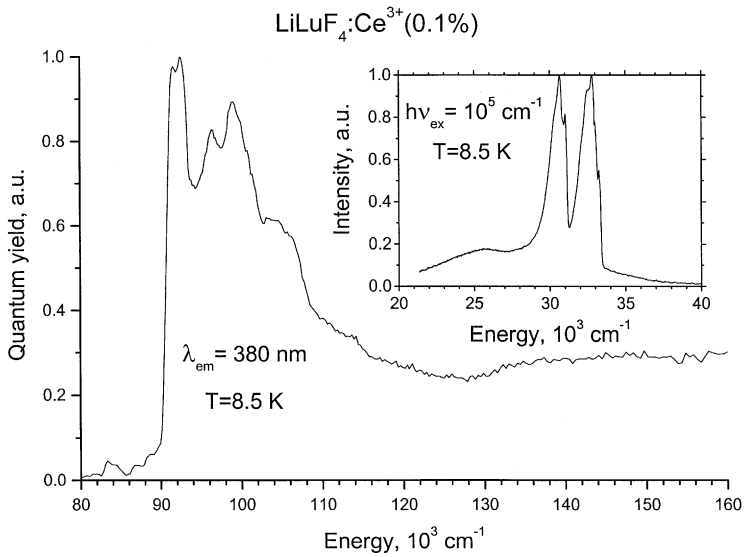

Fig. 7. Excitation spectrum of 380 nm (3.2 eV) emission from the $LiLuF_4$:Ce^{3+} crystal. In the insertion the emission spectrum of the $LiLuF_4$:Ce^{3+} crystal measured under the host excitation (with lower spectral resolution than those in Fig. 1) is shown.

380 nm luminescence overlaps by its short wavelength tail with the edge of Ce^{3+} 4f–5d absorption in $LiLuF_4$:Ce^{3+} and so, some energy transfer from STE to Ce^{3+} ions with the excitation of the latter to 5d levels can take place but with low efficiency. Since the decay of 380 nm STE emission is slow (see Fig. 5) the fraction of the slow component in excitation spectra in the region 11.2–12.5 eV is increased as confirmed by our measurements.

It should be especially mentioned that for the observation of $4f^{14}$–$4f^{13}5d$ transitions in Lu^{3+} it is necessary to have high concentration of Lu^{3+} in the crystal, in the best case 100% concentration in the stoichiometric compound, because of strong competition with other absorptions at photon energies >10 eV (80,000 cm^{-1}), in particular by the tail of excitonic absorption or by different defects and impurities. Since in the nominally pure (or slightly doped) stoichiometric compound $LiLuF_4$ most of the Lu^{3+} ions are not disturbed by defects or impurities, and interaction between neighboring excited Lu^{3+} ion in 5d state and non-excited Lu^{3+} ion in $^1S_0$ state for the completely filled 4f shell is very small, no strong inhomogeneous broadening of absorption (and emission) lines corresponding to $4f^{14}$–$4f^{13}5d$ transitions in Lu^{3+} is expected, and narrow zero-phonon lines can be observable.

4. Conclusions

As a result of low-temperature high-resolution VUV/UV spectroscopy measurements the well resolved fine structure due to zero-phonon lines was obtained in both excitation and emission spectra of $LiYF_4$:Ce^{3+} and $LiLuF_4$:Ce^{3+} crystals. For LuF_3:Ce^{3+} crystal no fine structure was detected in the spectra due to stronger electron–phonon interaction between the lowest 5d-state of Ce^{3+} and the lattice vibrations in this crystal. Under the host excitation of the $LiLuF_4$:Ce^{3+} crystal, the fine structure for high-energy emission band of Ce^{3+} ($5d$–$^2F_{5/2}$) was observed and interpreted as a result of weaker reabsorption effect, as compared to the region of Ce^{3+} 4f–5d absorption, due to small penetration depth for exciting radiation. The obtained zero-phonon-lines were assigned to crystal-field levels of $^2F_{7/2}$ and $^2F_{5/2}$ multiplets of Ce^{3+} in $LiLuF_4$. In the excitation spectrum of $LiLuF_4$:Ce^{3+} the narrow lines at $\sim$81,550 and $\sim$82,900 cm^{-1} were ascribed to zero-phonon lines due to $4f^{14}$–$4f^{13}5d$ transitions in Lu^{3+}. This result is considered as the first observation of zero-phonon lines for interconfigurational 4f–5d transitions in Lu^{3+}. The vibrational structure observed at the edge of Ce^{3+} 4f–5d transitions in $LiYF_4$:Ce^{3+} and $LiLuF_4$:Ce^{3+}, as well as at the edge of Lu^{3+} $4f^{14}$–$4f^{13}5d$ transitions in $LiLuF_4$:Ce^{3+} clearly shows that different vibrational modes are involved in electron–phonon interaction between the lowest 5d-state of Ce^{3+} and the lattice vibrations in different matrices and between the lowest 5d-states of Ce^{3+} or Lu^{3+} and lattice vibrations in the same matrix.

Acknowledgements

This work was supported by INTAS Grant 99-01350, NATO Collaborative Linkage Grant PST.CLG.976856, Graduiertenkolleg "Fields and localized atoms—Atoms and localized fields: Spectroscopy of localized atomic systems", IHP-Contract HPRI-CT-1999-00040/2001-00140 of the European Commission and Russian Federal Program "Integration" (Grant B0049).

References

[1] D.J. Ehrlich, P.F. Moulton, R.M. Osgood Jr., Opt. Lett. 4 (1979) 184.
[2] F. Okada, S. Togawa, K. Ohta, S. Koda, J. Appl. Phys. 75 (1994) 49.
[3] P. Rambaldi, R. Moncorge, J.P. Wolf, C. Pedrini, J.Y. Gesland, Opt. Commun. 146 (1998) 163.
[4] C.M. Combes, P. Dorenbos, C.W.E. van Eijk, C. Pedrini, J.Y. Gesland, Proceedings of the International Conference on Inorganic Scintillators and Their Applications, SCINT 95, Delft University Press, 1996, p. 396.
[5] C.M. Combes, P. Dorenbos, C.W.E. van Eijk, C. Pedrini, H.W. Den Hartog, J.Y. Gesland, P.A. Rodnyi, J. Lumin. 71 (1997) 65.
[6] E. Sarantopoulou, A.C. Cefalas, M.A. Dubinskii, C.A. Nicolaides, R.Yu. Abdulsabirov, S.L. Korableva,

A.K. Naumov, V.V. Semashko, Opt. Commun. 107 (1994) 104.
[7] J.C. Krupa, M. Queffelec, J. Alloys Compd. 250 (1997) 287.
[8] R.T. Wegh, H. Donker, A. Meijerink, Phys. Rev. B 57 (1998) R2025.
[9] J. Becker, J.Y. Gesland, N.Yu. Kirikova, J.C. Krupa, V.N. Makhov, M. Runne, M. Queffelec, T.V. Uvarova, G. Zimmerer, J. Lumin. 78 (1998) 91.
[10] N.M. Khaidukov, N.Yu. Kirikova, M. Kirm, J.C. Krupa, V.N. Makhov, E. Negodin, G. Zimmerer, Proc. SPIE 4766 (2002) 154.
[11] C.R. Ronda, J. Alloys Comp. 225 (1995) 534.
[12] R.T. Wegh, H. Donker, E.V.D. van Loef, K.D. Oskam, A. Meijerink, J. Lumin. 87–89 (2000) 1017.
[13] L. van Pieterson, M.F. Reid, R.T. Wegh, S. Soverna, A. Meijerink, Phys. Rev. B65 (2002) 045113.
[14] L. van Pieterson, M.F. Reid, G.W. Burdick, A. Meijerink, Phys. Rev. B65 (2002) 045114.
[15] L. van Pieterson, M.F. Reid, A. Meijerink, Phys. Rev. Lett. 88 (2002) 067405.
[16] E. Loh, Phys. Rev. 147 (1966) 332.
[17] G. Zimmerer, Nucl. Instr. Meth. A 308 (1991) 178.
[18] M. Louis, E. Simoni, S. Hubert, J.Y. Gesland, Opt. Mater. 4 (1995) 657.
[19] S. Salaun, M.T. Fornoni, A. Bulou, M. Rousseau, P. Simon, J.Y. Gesland, J. Phys.: Condens. Matt. 9 (1997) 6941.
[20] W.W. Moses, S.E. Derenzo, M.J. Weber, A.K. Ray-Chaudhuri, F. Cerrina, J. Lumin. 59 (1994) 89.
[21] T. Szczurek, M. Schlesinger, in: B. Jezowska-Trebiatowska, J. Legendziewich, W. Strek (Eds.), Rare Earth Spectroscopy, World Scientific, Singapore, 1985, p. 309.
[22] W. Blanc, C. Dujardin, J.C. Gacon, C. Pedrini, B. Moine, A.N. Belsky, I.A. Kamenskikh, M. Kirm, G. Zimmerer, Radiation Effects and Defects in Solids 150 (1999) 41.
[23] P. Dorenbos, J. Lumin. 91 (2000) 91.
[24] N.Yu. Kirikova, A.N. Belsky, B. Chassigneaux, J.C. Krupa, V.N. Makhov, M. Queffelec, unpublished.
[25] D. Bouttet, C. Dujardin, C. Pedrini, W. Brunat, D. Tran Minh Duc, Proceedings of the International Conference on Inorganic Scintillators and Their Applications SCINT'95, Delft, The Netherlands, August 28–September 1, 1995, Delft University Press, p. 111.
[26] P. Dorenbos, J. Phys.: Condens. Matt. 15 (2003) 8417.
[27] C.W. Theil, H. Cruguel, Y. Sun, G.J. Lapeyre, R.M. Macfarlane, R.W. Equall, R.L. Cone, J. Lumin. 94–95 (2001) 1.
[28] V.N. Makhov, N.M. Khaidukov, Nucl. Instr. Meth. A 308 (1991) 205.